The dependence of peak electron density in the ionosphere of Mars on solar irradiance

Z. Girazian[1] and P. Withers[1]

Received 4 February 2013; revised 6 March 2013; accepted 8 March 2013; published 26 May 2013.

[1] Previous studies of the Mars ionosphere have concluded that increased solar flux leads to increased peak electron densities. Many have described this relationship as $N_m \propto F^k$, where N_m is the peak electron density, F, the ionizing flux, is represented by either $F_{10.7}$ or $E_{10.7}$, and k is an exponent. The derived exponents have varied greatly, but have a mean value of $k \simeq 0.35$. Here, we explore this relationship using solar spectra measurements from the TIMED-SEE instrument and Mars Global Surveyor radio occultation data. Our derived exponents, $k \simeq 0.50$, are larger than those found by previous studies that used $F_{10.7}$ or $E_{10.7}$ and are close to the theoretical prediction of simplistic Chapman theory. **Citation:** Girazian, Z., and P. Withers (2013), The dependence of peak electron density in the ionosphere of Mars on solar irradiance, *Geophys. Res. Lett.*, *40*, 1960–1964, doi:10.1002/grl.50344.

1. Introduction

[2] The ionosphere of Mars is strongly influenced by the solar irradiance that maintains its dayside plasma. The ionosphere of Mars is also a source region for the escape of volatiles. Hence, determining how the ionosphere responds to changes in solar irradiance is crucial for understanding the present-day ionosphere and the long-term evolution of the atmosphere of Mars.

[3] The dayside ionosphere of Mars can be separated into a transport-controlled region ($\gtrsim$180 km) and a photochemically-controlled region ($\lesssim$180 km). Embedded in the photochemically controlled region is the M2 plasma layer ($\sim$ 140 km), produced primarily by extreme ultraviolet (EUV) solar photons with wavelengths (λ) less than 90 nm [*Martinis et al.*, 2003; *Withers*, 2009], and the less prominent M1 plasma layer ($\sim$ 110 km), produced by soft X-rays and subsequent electron collisions [*Rishbeth and Mendillo*, 2004; *Fox*, 2004]. This paper focuses on the M2 layer, where peak ion and electron densities occur.

[4] Spacecraft at Mars have obtained $\sim$ 7000 electron density profiles using radio occultation instruments [*Hinson et al.*, 1999, 2000; *Mendillo et al.*, 2003; *Pätzold et al.*, 2005] and more than 30,000 topside electron density profiles using the radar sounding instrument (MARSIS) on the Mars Express spacecraft [*Gurnett et al.*, 2005, 2008; *Němec et al.*, 2011]. In situ measurements are far less numerous but include two ion density and temperature profiles obtained by the Viking landers in 1976 [*Hanson et al.*, 1977] and one electron temperature profile obtained by a later analysis of Viking 1 data [*Hanson and Mantas*, 1988].

[5] Previous studies have tested how the peak electron density, N_m, depends on the ionizing solar flux, F, by deriving an exponent, k, using the following:

$$N_m \propto F^k. \tag{1}$$

Typically, the $F_{10.7}$ index, a measure of the solar radio flux at 10.7 cm, or the $E_{10.7}$ index, a measure of the integrated solar EUV energy flux from 1–105 nm [*Tobiska et al.*, 2000; *Tobiska*, 2001], is used as a direct proxy for F. *Hantsch and Bauer* [1990] used various ionospheric data sets from 1965 to 1980 to derive an exponent of 0.36. *Breus et al.* [2004], *Withers and Mendillo* [2005], *Zou et al.* [2006], and *Fox and Yeager* [2009] used Mars Global Surveyor (MGS) radio occultation data to derive exponents of 0.37 ± 0.06, 0.243 ± 0.031, 0.44, and 0.263 ± 0.0075, respectively. *Morgan et al.* [2008] and *Němec et al.* [2011] used MARSIS data to derive exponents of 0.30 ± 0.04 and 0.388 ± 0.003, respectively. These exponents vary greatly but have a mean value of $k \simeq 0.35$.

[6] The peak electron density is a well-defined quantity that can be obtained directly from ionospheric profiles. Reducing the ionizing flux to single number, however, is a nontrivial operation that is further confounded by the lack of solar irradiance measurements at Mars. In this paper, we use a proxy other than $F_{10.7}$ and $E_{10.7}$ to determine how peak electron density depends on the ionizing flux at Mars. Our proxy for F is calculated by integrating daily-averaged solar spectra measurements in the wavelength range that ionizes the dominant neutral at Mars, CO_2. Our derived exponents are compared to previous studies that have used $F_{10.7}$ or $E_{10.7}$ and put into physical context.

2. Procedure

[7] We began by retrieving the 5600 MGS electron density profiles from the NASA Planetary Data System (PDS). Figure 1 shows an example MGS profile. We discarded all near-terminator profiles with solar zenith angles (SZA) $> 80°$ to ensure day-night effects were eliminated.

[8] Peak electron densities, N_m, were obtained from the MGS profiles. The effects of varying SZA were eliminated by converting the obtained peak densities to subsolar (SZA = 0°) peak densities, N_0, using $N_0 = N_m \sqrt{Ch(X, \chi)}$, where χ is the SZA, $X = \frac{z+R}{H}$, z is the altitude above the surface, R = 3400 km is the planetary radius, H = 10 km is the neutral scale height, and $Ch(X, \chi)$ is the Chapman function [*Chapman*, 1931b], which reduces to sec χ for small χ [*Smith III and Smith*, 1972; *Withers*, 2009]. Although H is unknown, $Ch(X, \chi)$ is relatively insensitive to its precise

[1]Department of Astronomy, Boston University, Boston, Massachusetts, USA.

Corresponding author: Z. Girazian, Department of Astronomy, Boston University, Boston, MA, USA. (zrjg@bu.edu)

0094-8276/13/10.1002/grl.50344

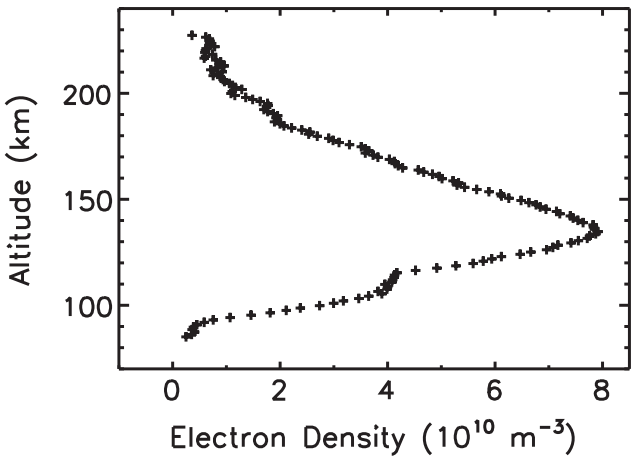

Figure 1. MGS profile 0361P19A from 26 December 2000 with SZA= 79.9°. The data points are shown by black crosses. The peak electron density from each MGS profile was obtained directly from the respective electron density profile.

value and *Withers* [2006] found that H is usually within 50% of 10 km. This dependence of peak density on SZA at Mars can be seen in *Morgan et al.* [2008], Figure 4, who used more than 10,000 MARSIS data points with SZA ranging from ∼ 5°–85°.

[9] The TIMED-SEE instrument [*Woods and Eparvier*, 2006] has obtained EUV solar spectra from Earth orbit since 22 January 2002. The instrument obtains 14–15 spectra measurements per day, which are then averaged. These daily-averaged spectra, or "Level 3 solar irradiance data", are available at http://lasp.colorado.edu/see/l3_data_page.html and are the spectra used throughout this paper.

[10] There are several possible measures of solar flux: the energy flux, the corresponding photon flux, and also a flux that describes the total number of ionization events. Due to secondary ionization processes, the number of ionization events per absorbed photon increases with increasing photon energy. We represent this using a "total number of ionizations" flux. This spectrum was calculated assuming that, after initial photoionization, the remaining energy contributes to secondary ionization, and that each secondary ionization requires 35 eV of energy [*Sheel et al.*, 2012; *Lollo et al.*, 2012]. Figure 2 shows an example TIMED-SEE energy flux spectrum with its corresponding photon flux and "total number of ionizations" spectrum.

[11] To apply Earth-based solar spectra measurements at Mars, the spectra were corrected from 1 AU values to account for the varying Mars-Sun distance. The spectra were also corrected for the non-uniformity of solar EUV irradiance across the solar surface by shifting the observation date of each MGS profile by an amount equal to (27 days) × (Mars-Sun-Earth angle/360°), where 27 days is solar rotation period. If the resultant date-shift was less than 7 days, then a single spectrum from the shifted date was obtained. If the resultant date-shift was seven or more days, then two spectra were obtained—one from before and one from after the observation, such that the Mars-facing side of the Sun during the MGS measurement was the same as the Earth-facing side of the Sun during both TIMED-SEE measurements. This correction is imperfect due to the neglect of temporal variations in solar flux. The PLOT_SEE.PRO

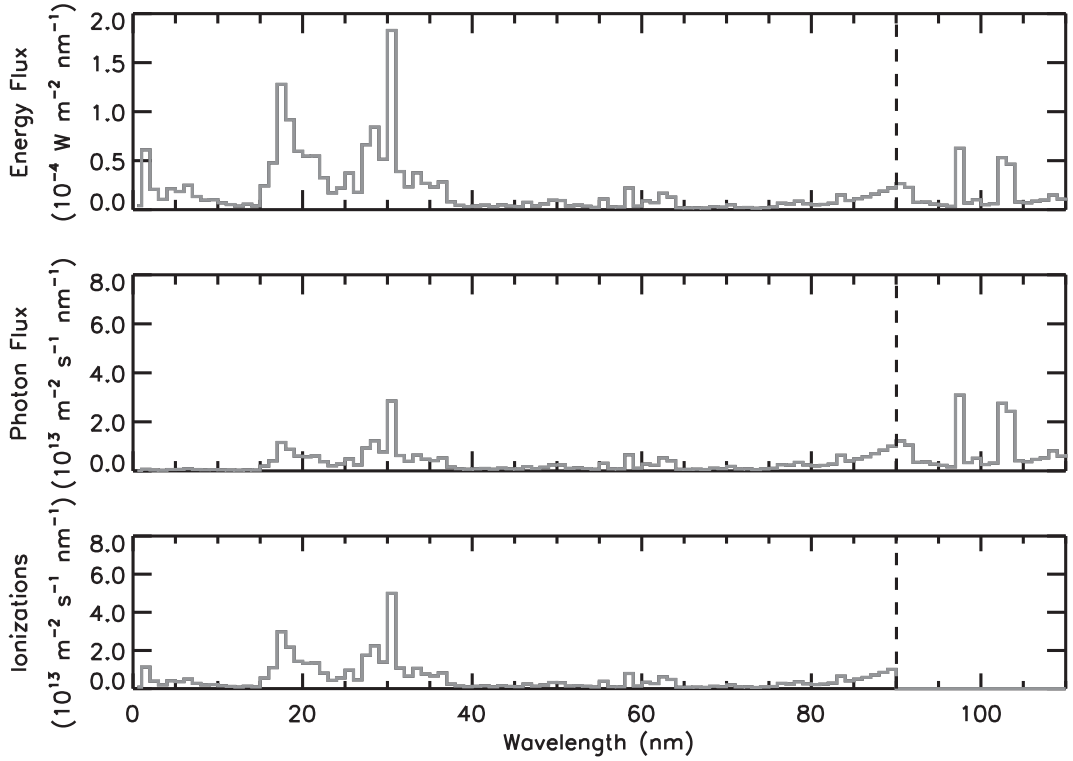

Figure 2. Example TIMED daily-averaged energy flux spectrum (top, F_e) with its corresponding photon flux spectrum (middle, F_p) and "total number of ionizations" spectrum (bottom, F_i) from 1 June 2003. The dashed line shows the longest wavelength photon (90.04 nm) that can ionize CO_2.

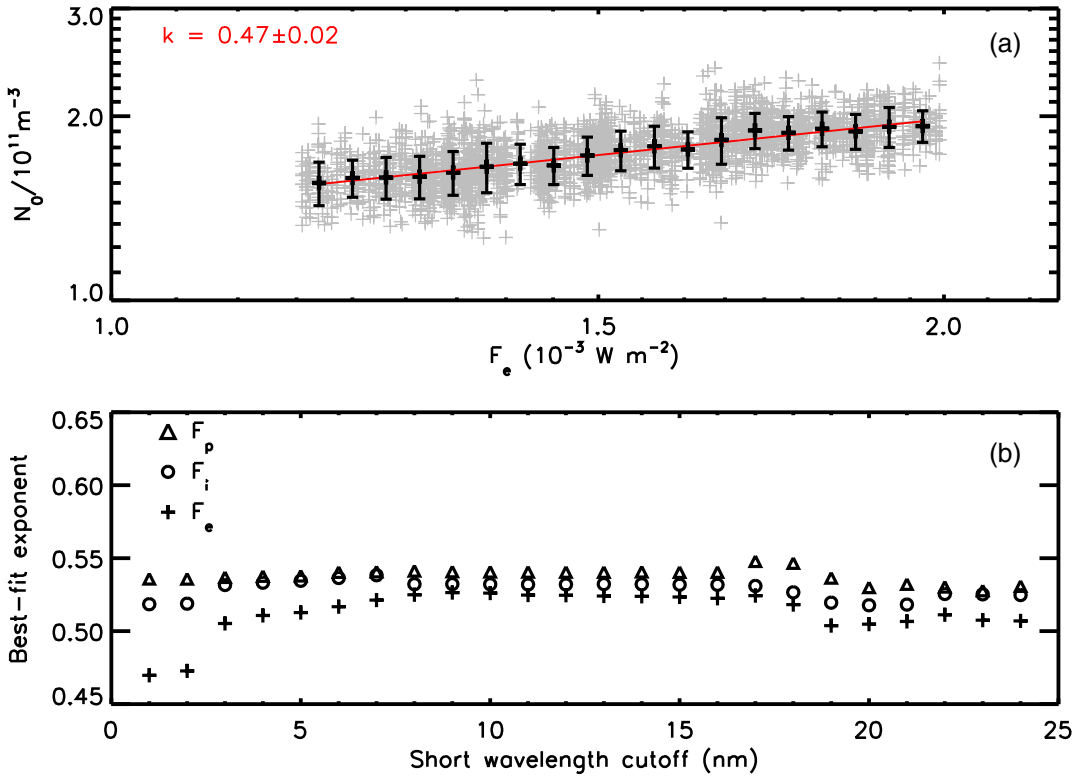

Figure 3. (a) A log-log plot showing the dependence of the peak electron density in the ionosphere of Mars on solar irradiance (F_e). Peak electron densities obtained from MGS profiles are shown by gray crosses. Average peak electron densities after binning and their respective 1σ uncertainties are shown by black crosses. The best fit line (equation (2)), shown in red, has an exponent of $k = 0.47 \pm 0.02$. (b) Best-fit exponents to equation (1) are shown for F_p, F_i, and F_e with different short wavelength cutoffs. The long wavelength cutoff is 90 nm in all cases. For short wavelength cutoffs larger than $\sim$ 3 nm, $k \simeq 0.50$, which is significantly larger than the $k \simeq 0.35$ derived by previous studies that used the $F_{10.7}$ and $E_{10.7}$ solar indices.

procedure, available at the TIMED-SEE website, performs these date-shifts and distance corrections. MGS profiles for which there is no TIMED-SEE data available were discarded during this process.

[12] The 2903 remaining MGS electron density profiles were obtained between 30 November 2002 and 29 April 2005. Their SZA range from 70.96° to 80.00° and their derived subsolar peak electron densities range from 1.26×10^{11} m^{-3} to 2.44×10^{11} m^{-3}, in agreement with *Fox and Yeager* [2009] and the numerous groups cited in *Withers* [2009].

[13] The date-shifted spectra corresponding to each MGS density profile were integrated from 1–90 nm. The long wavelength cutoff was chosen because the dominant neutral at Mars (> 95%), CO_2, is ionized by photons with $\lambda < 90.04$ nm [*Schunk and Nagy*, 2009]. If there were two date-shifted spectra (because the date-shift was longer than 7 days), they were both integrated from 1–90 nm and a weighted average was calculated. F_e is defined as the integrated energy flux from 1–90 nm, F_p as the corresponding integrated photon flux, and F_i as the corresponding integrated "total number of ionizations" flux. We use these as our representations of the ionizing flux, F, in equation (1).

[14] We divided the subsolar densities into 19 bins that have equal log-flux width, then used the mean densities of each bin to derive the best-fit value of the exponent k. The standard deviation of each bin provided 1σ uncertainties for the fit. The data were binned to compensate for the non-uniform distribution of data points.

3. Results and Discussion

[15] The result of the fit to equation (1) using F_e is

$$\ln\left[\frac{N_0}{10^{11}\ \mathrm{m}^{-3}}\right] = (0.47 \pm 0.02)\ln\left[\frac{F_{\mathrm{ion}}}{10^{-3}\ \mathrm{W\ m}^{-2}}\right] + (0.36 \pm 0.01) \quad (2)$$

and is shown in Figure 3. The fits using F_p and F_i resulted in derived exponents of $k = 0.54 \pm 0.02$ and $k = 0.52 \pm 0.02$, respectively. The exponents derived using our three proxies for the ionizing solar flux are all larger than the $k \simeq 0.35$ derived in previous studies (section 1) that used $F_{10.7}$ and $E_{10.7}$.

[16] To directly compare our results to previous studies, we repeated the analysis of section 2, including date-shifts and distance-corrections, using daily-averaged $F_{10.7}$ and $E_{10.7}$ indices obtained from the Solar Irradiance Platform (SIP) [*Tobiska et al.*, 2000] and derived exponents of $k = 0.32 \pm 0.02$ and $k = 0.42 \pm 0.01$ respectively. *Fox and Yeager* [2009] performed a similar analysis on MGS data using $F_{10.7}$ and found $k = 0.26 \pm 0.01$. These two exponents differ because *Fox and Yeager* [2009] used a different subset of MGS data and a different procedure to convert peak densities to subsolar peak densities.

[17] Reducing the ionizing flux at Mars to a single number is a challenge, and consequently, our three proxies are imperfect representations of the ionizing flux at Mars. First, our proxies include only wavelengths that ionize CO_2. Other species in the Martian atmosphere such as O, which is the dominant species at high altitudes, were neglected. Second, even if our proxies provided an accurate description of the total ionizing flux, they would not be proportional to the production rate of CO_2^+. This is because some of the incident flux goes into ionization of species other than CO_2 or various dissociative processes, and secondary ionization from energetic electrons has been approximated.

[18] Another challenge for reducing the ionizing flux to a single number is the dependence of the absorption and ionization cross sections of CO_2 on wavelength. These wavelength-dependent cross sections result in wavelength-dependent photon penetration depths and, as a result, the altitude of the maximum photoionization rate for a given wavelength is not necessarily the altitude of the M2 layer peak electron density. Nevertheless, as shown in Figure 2 of *Martinis et al.* [2003] and Figure 2 of *Fox and Yeager* [2006], maximum photoionization rates for photons with $15 \leq \lambda \leq 90$ nm occur at essentially the same altitude near the M2 peak. Photons with $\lambda < 15$ nm, however, penetrate deeper into the atmosphere, and their maximum photoionization rates occur at altitudes below the M2 peak. This complicates matters because our proxies are integrated over all wavelengths and incorrectly assume that the flux from each wavelength bin contributes equally to M2 peak photoionization. We explored this complication by deriving exponents using short wavelength cutoffs ranging from 1 to 24 nm. Figure 3 shows these derived exponents, all of which are $k \simeq 0.50$, unlike the $k \simeq 0.35$ found by previous studies that used $F_{10.7}$ or $E_{10.7}$. Therefore, although this wavelength dependence in cross section may change the resultant exponents, it does so in a way such that our overall conclusions are unaffected.

4. Conclusions

[19] The power-law exponent relating changes in subsolar peak electron density to changes in observed solar irradiance is approximately 0.50. For irradiance proxies based on the energy of ionizing solar flux (F_e), on the corresponding photon flux (F_p), and on the "total number of ionizations" flux (F_i), we obtained exponents of 0.47 ± 0.02, 0.54 ± 0.02, and 0.52 ± 0.02, respectively. There are valid arguments for preferring any one of these three potential irradiance proxies, yet all three are imperfect representations of the irradiance that controls peak electron density. F_p neglects the important process of secondary ionization and all three neglect variations in penetration depth with wavelength. In this application, all three proxies yield similar results.

[20] All three exponents are much larger than the mean exponent of $k \simeq 0.35$ reported by previous studies (section 1) that used $F_{10.7}$ or $E_{10.7}$ instead of solar flux observations. The exponents are also interestingly close to the $k = 0.50$ value that Chapman theory [*Chapman*, 1931a, 1931b; *Rishbeth and Garriott*, 1969] predicts. Chapman theory is a simplistic theory of the formation of ionospheric layers and many of its inherent assumptions are violated at Mars [*Withers*, 2009]. Our results imply that the dependence of peak electron density in the ionosphere of Mars on solar irradiance may be in better agreement with the prediction of Chapman theory than previously recognized.

[21] We postulate that this representation of the ionizing flux leads to more accurate predictions of the power-law exponent relating changes in subsolar peak electron density to changes in observed solar irradiance. Although $F_{10.7}$ has historically been used as a proxy for the solar EUV flux due to the lack of EUV observations, scientists have long recognized that $F_{10.7}$ is not directly proportional to the ionizing solar flux, even at Earth. Although $E_{10.7}$ and F_e are similar, $E_{10.7}$ includes wavelengths greater than 90 nm, which do not ionize the dominant neutral at Mars, CO_2. Figure 2 shows significant emission features in this region of the spectrum from 90–105 nm. These extra sources of flux that are included in $E_{10.7}$—but do not contribute to ionization of CO_2—explain why $E_{10.7}$ inaccurately represent the ionizing flux at Mars. This method for calculating a proxy for the ionizing flux can be tailored to the compositions of different planetary atmospheres, although it is limited by the scarcity of EUV observations.

[22] **Acknowledgments.** The work was partially supported by NASA awards NNX08AN56G, NNX08AP96G, and NNX12AJ39G. We acknowledge two helpful reviewers and discussions with Katy Fallows.

References

Breus, T. K., A. M. Krymskii, D. H. Crider, N. F. Ness, D. Hinson, and K. K. Barashyan (2004), Effect of the solar radiation in the topside atmosphere/ionosphere of Mars: Mars Global Surveyor observations, *J. Geophys. Res.*, *109*, A09310, doi:10.1029/2004JA010431.

Chapman, S. (1931a), The absorption and dissociative or ionizing effect of monochromatic radiation in an atmosphere on a rotating Earth, *Proc. Phys. Soc.*, *43*, 26–45, doi:10.1088/0959-5309/43/1/305.

Chapman, S. (1931b), The absorption and dissociative or ionizing effect of monochromatic radiation in an atmosphere on a rotating Earth. Part II. Grazing incidence, *Proc. Phys. Soc.*, *43*, 483–501, doi:10.1088/0959-5309/43/5/302.

Fox, J. L. (2004), Response of the Martian thermosphere/ionosphere to enhanced fluxes of solar soft X-rays, *J. Geophys. Res.*, *109*, A11310, doi:10.1029/2004JA010380.

Fox, J. L., and K. E. Yeager (2006), Morphology of the near-terminator Martian ionosphere: A comparison of models and data, *J. Geophys. Res.*, *111*, A10309, doi:10.1029/2006JA011697.

Fox, J. L., and K. E. Yeager (2009), MGS electron density profiles: Analysis of the peak magnitudes, *Icarus*, *200*, 468–479, doi:10.1016/j.icarus.2008.12.002.

Gurnett, D. A., et al. (2005), Radar soundings of the ionosphere of Mars, *Science*, *310*, 1929–1933, doi:10.1126/science.1121868.

Gurnett, D. A., et al. (2008), An overview of radar soundings of the Martian ionosphere from the Mars Express spacecraft, *Adv. Space Res.*, *41*, 1335–1346, doi:10.1016/j.asr.2007.01.062.

Hanson, W. B., and G. P. Mantas (1988), Viking electron temperature measurements—Evidence for a magnetic field in the Martian ionosphere, *J. Geophys. Res.*, *93*, 7538–7544, doi:10.1029/JA093iA07p07538.

Hanson, W. B., S. Sanatani, and D. R. Zuccaro (1977), The Martian ionosphere as observed by the Viking Retarding Potential Analyzers, *J. Geophys. Res.*, *82*, 4351–4363, doi:10.1029/JS082i028p04351.

Hantsch, M. H., and S. J. Bauer (1990), Solar control of the Mars ionosphere, *Planet. Space Sci.*, *38*, 539–542, doi:10.1016/0032-0633(90)90146-H.

Hinson, D. P., R. A. Simpson, J. D. Twicken, G. L. Tyler, and F. M. Flasar (1999), Initial results from radio occultation measurements with Mars Global Surveyor, *J. Geophys. Res.*, *104*, 26,997–27,012, doi:10.1029/1999JE001069.

Hinson, D. P., R. A. Simpson, J. D. Twicken, G. L. Tyler, and F. M. Flasar (2000), Erratum: Initial results from radio occultation measurements with Mars Global Surveyor, *J. Geophys. Res.*, *105*, 1717–1718, doi:10.1029/1999JE900045.

Lollo, A., P. Withers, K. Fallows, Z. Girazian, M. Matta, and P. C. Chamberlin (2012), Numerical simulations of the ionosphere of Mars during a solar flare, *J. Geophys. Res.*, *117*, A05314, doi:10.1029/2011JA017399.

Martinis, C. R., J. K. Wilson, and M. J. Mendillo (2003), Modeling day-to-day ionospheric variability on Mars, *J. Geophys. Res.*, *108*, 1383, doi: 10.1029/2003JA009973.

Mendillo, M., S. Smith, J. Wroten, H. Rishbeth, and D. Hinson (2003), Simultaneous ionospheric variability on Earth and Mars, *J. Geophys. Res.*, *108*, 1432, doi:10.1029/2003JA009961.

Morgan, D. D., D. A. Gurnett, D. L. Kirchner, J. L. Fox, E. Nielsen, and J. J. Plaut (2008), Variation of the Martian ionospheric electron density from Mars Express radar soundings, *J. Geophys. Res.*, *113*, A09303, doi: 10.1029/2008JA013313.

Němec, F., D. D. Morgan, D. A. Gurnett, F. Duru, and V. Truhlík (2011), Dayside ionosphere of Mars: Empirical model based on data from the MARSIS instrument, *J. Geophys. Res.*, *116*, E07003, doi: 10.1029/2010JE003789.

Pätzold, M., S. Tellmann, B. Häusler, D. Hinson, R. Schaa, and G. L. Tyler (2005), A sporadic third layer in the ionosphere of Mars, *Science*, *310*, 837–839, doi:10.1126/science.1117755.

Rishbeth, H., and O. K. Garriott (1969), *Introduction to Ionospheric Physics*, pp. 89–94, Academic Press, New York.

Rishbeth, H., and M. Mendillo (2004), Ionospheric layers of Mars and Earth, *Planet. Space Sci.*, *52*, 849–852, doi:10.1016/j.pss.2004.02.007.

Schunk, R. W., and A. F. Nagy (2009), *Ionospheres*, 261 p., Cambridge University Press, New York.

Sheel, V., S. A. Haider, P. Withers, K. Kozarev, I. Jun, S. Kang, G. Gronoff, and C. Simon Wedlund (2012), Numerical simulation of the effects of a solar energetic particle event on the ionosphere of Mars, *J. Geophys. Res.*, *117*, A05312, doi:10.1029/2011JA017455.

Smith III, F. L., and C. Smith (1972), Numerical evaluation of Chapman's grazing incidence integral Ch(X,χ), *J. Geophys. Res.*, *77*, 3592–3597, doi:10.1029/JA077i019p03592.

Tobiska, W. K. (2001), Validating the solar EUV proxy, $E_{10.7}$, *J. Geophys. Res.*, *106*, 29,969–29,978, doi:10.1029/2000JA000210.

Tobiska, W. K., T. Woods, F. Eparvier, R. Vierreck, L. Floyd, D. Bouwer, G. Rottman, and O. R. White (2000), The SOLAR2000 empirical solar irradiance model and forecast tool, *J. Atmos. Solar-Terr. Phys.*, *62*, 1233–1250, doi:10.1016/S1364-6826(00)00070-5.

Withers, P. (2006), Mars Global Surveyor and Mars Odyssey accelerometer observations of the Martian upper atmosphere during aerobraking, *Geophys. Res. Lett.*, *33*, L02201, doi:10.1029/2005GL024447.

Withers, P. (2009), A review of observed variability in the dayside ionosphere of Mars, *Adv. Space Res.*, *44*, 277–307, doi: 10.1016/j.asr.2009.04.027.

Withers, P., and M. Mendillo (2005), Response of peak electron densities in the Martian ionosphere to day-to-day changes in solar flux due to solar rotation, *Planet. Space Sci.*, *53*, 1401–1418, doi: 10.1016/j.pss.2005.07.010.

Woods, T. N., and F. G. Eparvier (2006), Solar ultraviolet variability during the TIMED mission, *Adv. Space Res.*, *37*, 219–224, doi: 10.1016/j.asr.2004.10.006.

Zou, H., J.-S. Wang, and E. Nielsen (2006), Reevaluating the relationship between the Martian ionospheric peak density and the solar radiation, *J. Geophys. Res.*, *111*, A07305, doi:10.1029/2005JA011580.